

# On the normal detonation shock velocity - curvature relationship for materials with large activation energy

Jin Yao, D. Scott Stewart\*

September 27, 1993

## Abstract

We derive the normal detonation shock velocity, curvature relation for a near-Chapman-Jouguet detonation, for an explosive material with Arrhenius kinetics and a large activation energy. Large activation energy asymptotics are used to develop an explicit exponential formula relating the shock curvature  $\kappa$  to the normal detonation shock speed,  $D_n$ . In this case, the  $D_n - \kappa$  relation is multi-valued and has a turning point with a critical curvature  $\kappa_{cr}$  such that for  $\kappa > \kappa_{cr}$ , the possibility of detonation extinction arises. The asymptotic formula is in excellent agreement with the exact solution found by numerical shooting procedure.

## 1 Introduction

In this paper we carry out a calculation that derives the normal detonation shock velocity - curvature relationship for materials with large activation energy. The analysis is valid for detonations that are near-Chapman-Jouguet (CJ), with equilibrium reaction zones that are sonic, or near-sonic. In addition the radius of curvature of the detonation shock is assumed to be large compared to a characteristic one-dimensional (1D) reaction zone thickness.

---

\*Theoretical and Applied Mechanics, University of Illinois, Urbana, Illinois, issued as TAM Report No. 727, UIIU-ENG-93-6025

This relation, called the  $D_n - \kappa$  relation, is an intrinsic property of an explosive material and can be derived if the material in question is modeled by the reactive Euler equations, [1], [2], [3]. If the  $D_n - \kappa$  relation is known, it can be used to propagate the detonation shock by means of corrected Huygen's construction. The shock propagates as a surface under the influence of its curvature.

Specifically we illustrate this result for a standard explosive model that is especially suited for gases, and can be used with care to model condensed explosives. The material is assumed to have a polytropic equation of state, ideal gas law, and Arrhenius kinetics for a simple, forward, exothermic energy release.

A similar problem was recently considered in [6], to which the reader is referred for further background. We use a notation that is essentially the same as that paper, here. Some of the results in [6] were aimed at examining the influence of state sensitivity of the reaction rate, on the effect of the curvature. A basic property of the  $D_n - \kappa$  relation is that for positive shock curvature (concave in the direction of a shock normal that points in the direction of the unburnt material), the detonation velocity generally decreases with increasing curvature. In the simplest examples, where the rate-state dependence is not highly sensitive, the  $D_n - \kappa$  relation is essentially linear.

However, it was thought that for sufficient state sensitivity of the pre-multiplying term in the reaction rate, that a critical curvature  $\kappa_{cr}$  could be calculated analytically, and for shock curvatures  $\kappa > \kappa_{cr}$ , quasi-steady, quasi-1D propagation would not be possible. In this case the  $D_n - \kappa$  relation would be multi-valued and have a turning point and the possibility of detonation extinction would arise. This multi-valued response has been observed in the numerical solution for the  $D_n - \kappa$  relation for models that describe non-ideal explosives, [4]. A similar multi-valued response was calculated in [5] for a non-physical model of a kinetic rate law that was explicitly sensitive to perturbations of the shock velocity.

The recent work in [6], did not explicitly consider the appropriate distinguished asymptotic limit of small shock curvature, measured on the correct induction zone length when the activation energy is large. Hence the multi-valued character of the  $D_n - \kappa$  relation was not found. We give that analysis here in a large activation energy limit, and thus provide the details of a (after the fact) straightforward exercise in large activation energy asymptotics. We give an explicit formulas for the  $D_n - \kappa$  relation that are sure to be used

in further numerical and stability studies, and for further extensions of the broader theory of Detonation Shock Dynamics.

In what follows, in section 2, we briefly restate the basic reduced problem with emphasis on the special case when the problem can be posed entirely in the particle velocity,  $U$  reaction progress variable,  $\lambda$  plane. In section 3, we carry out the asymptotic analysis and derive the  $D_n - \kappa$  relation. In section 4. we compare the analytical and the exact (numerically computed) results.

## 2 The reduced problem

### 2.1 Scaling

The dimensional scales, for the density  $\rho$ , pressure  $p$ , shock attached normal particle velocity,  $U$ , length  $n$  and time scales are:

$$\rho_0, \rho_0 D_{CJ}^2, D_{CJ}, \ell_c, \ell_c/D_{CJ},$$

where the length  $\ell_c$  scale is as yet unspecified. The progress variable  $\lambda$  is zero at the shock and one when the reaction is completed. Near-CJ, quasi-1D, quasi-steady detonations have the property that

$$\kappa \ell_c \ll 1, \text{ and } D \sim D_{CJ}.$$

### 2.2 Quasi-steady, quasi-1D, equations

Following [6] the quasi-steady, quasi-1D, equations are the reduced Euler equations in the streamwise direction, with a correction for the total shock curvature,  $\kappa$ . Here  $e$  is the specific internal energy and we write

$$\frac{\partial(\rho U)}{\partial n} + \kappa \rho (U + D_n) = 0, \quad (1)$$

$$U \frac{\partial U}{\partial n} + \frac{1}{\rho} \frac{\partial p}{\partial n} = 0, \quad (2)$$

$$\frac{\partial e}{\partial n} - \frac{p}{\rho^2} \frac{\partial \rho}{\partial n} = 0, \quad (3)$$

$$U \frac{\partial \lambda}{\partial n} = r. \quad (4)$$

The strong shock boundary condition hold at  $n = 0$  and are given by

$$U = -\frac{\gamma-1}{\gamma+1}D_n, \quad \rho = \rho_0 \frac{\gamma+1}{\gamma-1}, \quad p = \frac{2}{\gamma+1}\rho_0 D_n^2, \quad \lambda = 0, \quad (5)$$

at the shock at  $n = 0$ .  $U \equiv u_n^\ell - D_n$  is the shock frame normal velocity,  $u^\ell$  is the lab-frame normal particle velocity,  $D_n$  is the normal shock velocity,  $n$  is the coordinate in the direction normal to the shock, and positive in the direction toward the unburnt material.

In addition we assume the polytropic equation of state

$$e = \frac{1}{\gamma-1} \frac{p}{\rho} - Q\lambda,$$

where  $\gamma$  is the polytropic exponent and  $Q$  is the heat of combustion. The sound speed  $c$  is given by

$$c^2 = \gamma \frac{p}{\rho} = \gamma RT,$$

where  $T$  is the temperature. In our calculations we use  $c^2$ . An Arrhenius form for the reaction rate is assumed,

$$r = k(1-\lambda)^\nu e^{-E/RT} = k(1-\lambda)^\nu e^{-\gamma E/c^2},$$

where  $k$  is the rate premultiplier,  $\nu$  is the reaction depletion exponent, and  $E$  is the activation energy.

In what follows, we use the scalings identified above and consider dimensionless quantities as those without any superscripts, and express dimensional quantities with a tilde superscript. The equations are essentially unchanged. Some parameters change their definitions slightly. For example, where  $\tilde{Q}$  appears it is replaced by  $q = \tilde{Q}/\tilde{D}_{CJ}^2$ . We also use the strong shock approximation, which shows that  $\tilde{D}_{CJ}^2 = 2(\gamma^2 - 1)\tilde{Q}$ , so that  $q = 1/(2(\gamma^2 - 1))$ . The scaled activation energy is replaced by  $\theta = \gamma\tilde{E}/\tilde{D}_{CJ}^2$ .

### 2.3 Formulation in $U - \lambda$ plane

The  $U - \lambda$  plane was used to discuss slightly divergent detonation in Fickett and Davis, [7] and in used to discuss the  $D_n - \kappa$  relation in [1] and [6], for example. The scaled formulation is for  $U(\lambda)$ , results in the "master equation" given by

$$\frac{dU}{d\lambda} = \frac{U\Phi}{r\eta} = U \frac{[q(\gamma - 1) - c^2(\kappa/r)(U + D_n)]}{(c^2 - U^2)}, \quad (6)$$

subject to the shock boundary condition

$$U = -\frac{\gamma - 1}{\gamma + 1} D_n. \quad (7)$$

In equation (6) we define the thermicity parameter as

$$\Phi \equiv (\gamma - 1)qr - c^2\kappa(U + D_n). \quad (8)$$

A total energy integral (Bernoulli's equation) is available that holds throughout the structure to  $O(\kappa)$  and gives a formula for  $c^2$  in terms of  $D_n, U$  and  $\lambda$  as

$$c^2 = \frac{\gamma - 1}{2}(D_n^2 - U^2) + q(\gamma - 1)\lambda. \quad (9)$$

Finally the sonic parameter can be identified as

$$\eta \equiv c^2 - U^2 = \frac{\gamma - 1}{2}D_n^2 - \frac{\gamma + 1}{2}U^2 + q(\gamma - 1)\lambda \quad (10)$$

The second condition that we must apply is consistent passage through the sonic locus, which is called the "generalized CJ condition". We turn to that next.

### 2.4 The generalized CJ conditions

The generalized CJ condition was identified in Wood and Kirkwood's original paper on the relation between detonation velocity and curvature, [8]. The condition is essentially seen from the master equation (6), in that when the flow is sonic, (i.e.  $\eta = 0$ ) then the thermicity parameter,  $\Phi$  must vanish simultaneously. This is a compatibility condition that must be hold at the

sonic point, otherwise the formulation is inconsistent and a solution cannot be described by the equations listed above.

Thus the generalized CJ conditions at a sonic point (or surface) in the flow are given by the pair of conditions that must hold simultaneously

$$U^2 = c^2, \text{ and } \Phi = (\gamma - 1)qr - c^2\kappa(U + D_n) = 0. \quad (11)$$

## 2.5 Induction-zone length scale

Without regard to the specification of the length scale, the dimensionless reaction rate and curvature, are given by the formula

$$r = \tilde{r} \frac{\tilde{\ell}_c}{\tilde{D}_{CJ}}, \quad \tilde{r} = \tilde{k}(1 - \lambda)^\nu \exp(-\theta/c^2),$$

$$\kappa = \tilde{k} \tilde{\ell}_c.$$

If we consider the curvature measured on the *induction* length scale (IZ)

$$\tilde{\ell}_c = \tilde{k}^{-1} \tilde{D}_{CJ} \frac{1}{\theta} \exp(\theta/c_s^2), \quad (12)$$

then we find

$$r = \frac{1}{\theta} \exp \left[ \theta \left( \frac{1}{c_s^2} - \frac{1}{c^2} \right) \right] (1 - \lambda)^\nu.$$

Note that  $c_s^2 = 2\gamma(\gamma-1)/(\gamma+1)^2$ . Further, we consider curvature changes and shock velocity changes that are at the same order, so that the perturbations of  $D_n$ , and  $\kappa$  are  $O(1/\theta)$ . Thus we write

$$\kappa = \frac{\hat{\kappa}}{\theta} \quad (13)$$

where  $\hat{\kappa} \sim O(1)$ .

This limit is different from that considered in [6], where instead a successive limit  $\theta \rightarrow \infty$  ( $\kappa \rightarrow 0$ ) was considered. Here we consider a *distinguished limit*  $\theta \rightarrow \infty$ , with  $\kappa$ , measured on the induction length scale, such that  $\kappa \sim \hat{\kappa}/\theta$ , with  $\hat{\kappa} \sim O(1)$ .

The standard analysis for a state-insensitive rate, found in [1] and [6], for example, identifies a main-reaction-layer (MRL) and a transonic layer (TSL). The essential feature of the MRL is that it is nominally 1D and for rate-state insensitive materials, the MRL is immediately adjacent to the shock. The TSL describes the flow in the neighborhood of the sonic point.

In contrast, this analysis has an induction-zone layer (IZ) adjacent to the shock followed by a MRL. The IZ has the familiar properties of an induction zone; small reaction depletion and large state sensitivity of the reaction rate to perturbations (in this case controlled by shock speed and curvature changes). The TSL is of exponentially small order and is imbedded within the MRL.

### 3 Asymptotic Analysis

#### 3.1 Induction-zone layer

In the induction zone,  $O(1/\theta)$  perturbations in the shock speed  $D_n$ , induce reactant consumption changes at  $O(1/\theta)$  and interact with curvature effects at  $O(1/\theta)$ . Thus we are led to the expansions

$$D = 1 + \kappa D^{(1)} + \dots$$

$$U^{IZ} = -\frac{\gamma - 1}{\gamma + 1} + \kappa U^{(1)} + \dots,$$

and the independent variable in the IZ is

$$\lambda = \frac{z}{\theta}.$$

The IZ expansion, substituted into (6) leads to an equation for  $U^{(1)}$  of the form

$$\hat{\kappa} \frac{dU^{(1)}}{dz} = - \left[ q(\gamma - 1) - \frac{\kappa}{r} c^2 (U + D_n) \right]^{(0)},$$

where the approximation of the right hand side follows below. In particular  $\kappa/r$  is approximated by

$$\frac{\kappa}{r} = \hat{\kappa} \exp \left[ -\frac{\theta}{c_s^2} + \frac{\theta}{c^2} \right]$$

where

$$c^2 = c_s^2 + (\gamma - 1)\kappa \left( D_n^{(1)} + \frac{\gamma - 1}{\gamma + 1} U^{(1)} \right) + \frac{\lambda}{2(\gamma + 1)} + \dots$$

The equation for  $U^{(1)}$  is

$$\hat{\kappa} \frac{dU^{(1)}}{dz} = \frac{1}{2(\gamma + 1)} \times \left\{ \frac{8\gamma(\gamma - 1)}{(\gamma + 1)^2} \hat{\kappa} \exp \left[ c_s^{-4} \left[ \hat{\kappa}(\gamma - 1) \left( D_n^{(1)} + \frac{\gamma - 1}{\gamma + 1} U^{(1)} \right) + \frac{1}{2} \frac{z}{\gamma + 1} \right] \right] - 1 \right\}. \quad (14)$$

The boundary shock boundary condition for this problem is given by (7). The other boundary condition, comes from consideration of matching the IZ - layer with the MRL layer.

### 3.2 The MRL

Here we consider the second layer in the structure of the wave, namely the MRL. Also we point out the essential absence of a TSL, in the sense that a separate analysis of the TSL is not needed to suitably approximate the flow through the sonic point. In particular, to show this we first consider the flow near the generalized CJ point.

From conditions (11) we find that at the sonic point  $\lambda$  is exponentially close to 1. To see this, one only need consider the form of the premultiplying term in rate function near the sonic point. To leading order the sound speed is

$$c_{sonic}^2 = \frac{\gamma^2}{(\gamma + 1)^2} > c_{shock}^2 = \frac{2\gamma(\gamma - 1)}{(\gamma + 1)^2}.$$

Note that this inequality is valid only for  $\gamma < 2$  and from here on we make that assumption. Hence the rate is premultiplied by



$$\exp \left[ \theta \left( \frac{1}{c_{shock}^2} - \frac{1}{c_{sonic}^2} \right) \right]$$

which is exponentially large and forces  $(1 - \lambda)$  to be an exponentially small term (e.s.t.), since the generalized CJ conditions, require that  $\kappa/r$  be  $O(1)$ .

Since  $\lambda = 1 - e.s.t.$  to all algebraic orders in  $1/\theta$ , then the conditions  $\eta = U^2 - c^2 = 0$ , and  $\lambda = 1$ , is all that is needed. One can use the value  $\lambda = 1$  to obtain a formula for  $c^2$  (from the energy integral) only in terms of  $U$  and  $D_n$ . The terms that normally result from small reaction are e.s.t and do not enter into the analysis at an algebraic order. If we represent the expansion near the sonic point as

$$U = -\frac{\gamma}{\gamma + 1} + U', \text{ and } D_n = 1 + D'_n,$$

the generalized CJ condition for the leading order algebraic perturbations must satisfy,

$$U' = -\frac{\gamma - 1}{\gamma} D'_n,$$

at  $\lambda = 1$  in the  $U - \lambda$  - plane. Thus the TSL layer is in some sense is degenerate, exponentially small, and not really necessary for this analysis.

Another way to explain the same point is to notice that the ratio  $\kappa/r$  is necessarily exponentially small, outside the induction zone, since the temperature and sound speed at leading order rises as we travel through the reaction zone towards the sonic plane. Equation (6) then reduces to the plane, 1D, CJ, detonation structure equation, since curvature effects are absent. The only difference is then that since the MRL is not directly adjacent to the shock, one does not immediately apply the shock boundary condition, rather the MRL carries the perturbation produced by the IZ - layer.

In the MRL we are then exactly led to the same analysis as in found in [1] and [6]. We will denote the perturbation of the MRL solution with a lower case  $u$  and note that to leading order the solution must by necessity be the plane 1D solution. Thus we expand the MRL solution as

$$U^{MRL} = -\frac{\gamma - \ell}{\gamma + 1} + \kappa u^{(1)}(\ell) + \dots,$$

where

$$\ell = \sqrt{1 - \lambda},$$

and from the master equation and the expansion for  $D$ , we obtain the equation for  $u^{(1)}$

$$\frac{du^{(1)}}{d\ell} + \frac{\gamma}{\ell(\gamma - \ell)}u^{(1)} = -\frac{(\gamma - 1)}{\ell(\gamma - \ell)}D^{(1)}.$$

The solution is

$$u^{(1)} = A - \frac{\gamma}{\ell} \left[ A + \frac{(\gamma - 1)}{\gamma} D^{(1)} \right],$$

where  $A$  is the arbitrary constant of integration, for the homogenous solution for  $u^{(1)}$ . Note that application of the TSL condition, that  $U' = -[(\gamma - 1)/\gamma]D'_n$ , forces use to choose  $A = -(\gamma - 1)/\gamma D_n^{(1)}$ , hence we conclude that to the first correction in the MRL, that the solution is simply a constant,

$$u^{(1)} = -\frac{\gamma - 1}{\gamma} D_n^{(1)}. \quad (15)$$

This last condition can now be used as the second boundary condition that in turn closes the formulation of the IZ - layer.

### 3.3 The $D_n - \kappa$ relation for large activation energy

Equation (14) is simplified and can be integrated by introducing the variable  $w$

$$U^{(1)} = w - \frac{z}{2(\gamma + 1)\hat{\kappa}},$$

and now the equation for  $w$  can be written more simply as

$$\frac{dw}{dz} = \sigma \exp[-\hat{\kappa}(\alpha D_n^{(1)} + \beta w)] \exp[-\delta z], \quad (16)$$

subject to the two boundary conditions,

$$w = -\frac{\gamma - 1}{\gamma + 1} D_n^{(1)},$$

at the shock at  $z = 0$ , and

$$w = -\frac{\gamma - 1}{\gamma} D_n^{(1)},$$

as  $z \rightarrow \infty$ , which is the matching boundary condition that describes how the IZ merges into the MRL. The constants  $\sigma, \alpha, \beta$  and  $\delta$  are all defined by in terms of  $\gamma$  as

$$\begin{aligned} \sigma &= \frac{4\gamma(\gamma - 1)}{(\gamma + 1)^3}, \quad \alpha = \frac{(\gamma + 1)^4}{4\gamma^2(\gamma - 1)}, \\ \beta &= \frac{(\gamma + 1)^3}{4\gamma^2}, \quad \delta = \frac{(\gamma + 1)^2(3 - \gamma)}{8\gamma(\gamma - 1)^2}. \end{aligned} \quad (17)$$

Equation (16) can be integrated simply, since it is separable, and the successive application of the two boundary condition listed above, first determine the integration constant, and then provide a constraint, between  $\hat{\kappa}$  and  $D_n^{(1)}$ , i.e. the  $D_n - \kappa$  relation.

In particular, one obtains directly

$$e^{a\hat{\kappa}D_n^{(1)}} + d\hat{\kappa}e^{-b\hat{\kappa}D_n^{(1)}} = 1, \quad (18)$$

where  $a, b$  and  $d$  are defined by

$$a = \frac{(\gamma + 1)^2(\gamma - 1)}{4\gamma^3}, \quad b = \frac{(\gamma + 1)^3(3\gamma - 1)}{4\gamma^3(\gamma - 1)}, \quad d = \frac{8(\gamma - 1)^3}{(3 - \gamma)(\gamma + 1)^2}.$$

Using the leading order results that  $\hat{\kappa}D_n^{(1)} = \theta(D_n - 1)$ , and  $\kappa = \hat{\kappa}/\theta$ , results in the explicit formula for  $\kappa$  as a function of  $D_n - 1$ , namely

$$\kappa = \frac{e^{b\theta(D_n-1)}}{d\theta} (1 - e^{a\theta(D_n-1)}). \quad (19)$$

The critical values of the  $D_n$  and  $\kappa$ , at the turning point, according to formula (19) are given by

$$(D_n)_{cr} = 1 + \frac{1}{a\theta} [\ln b - \ln(a + b)], \quad \kappa_{cr} = \frac{1}{\theta} \frac{a}{(a + b)d} \left( \frac{b}{a + b} \right)^{b/a}. \quad (20)$$

The dimensional formula can be constructed quite simply by reintroducing the dimensional scales, and making the replacements

$$D_n = \frac{\tilde{D}_n}{\tilde{D}_{CJ}}, \quad \kappa = \tilde{\kappa} \tilde{\ell}_c,$$

where

$$\tilde{\ell}_c = \tilde{k}^{-1} \tilde{D}_{CJ} \frac{1}{\theta} \exp(\theta/c_s^2),$$

with

$$\theta = \frac{\gamma \tilde{E}}{\tilde{D}_{CJ}^2}, \quad \text{and } c_s^2 = 2\gamma(\gamma - 1)/(\gamma + 1)^2.$$

## 4 Properties and comparison of the asymptotic and exact solutions

### 4.1 Properties of the $D_n - \kappa$ relation

Figure 1, shows a plot of the reduced  $D_n - \kappa$  relation, in terms of  $\hat{\kappa} D_n^{(1)}$  versus  $\hat{\kappa}$  from formula (18) for  $\gamma = 1.2$  to illustrate that the turning point, is contained within our approximations.

It is also worth pointing out that the depletion parameter,  $\nu$  seems to have no effect on this analysis, at least to the order that we have carried out so far. The principle reason for this is that the analysis is dominated by the behavior in the IZ, and the depletion exponent plays no role there since  $\lambda$  is close to zero, and  $(1 - \lambda)^\nu$  is close to one.

Figure 2 shows a comparison of the asymptotic formula for the  $D_n - \kappa$  relation evaluated for finite values of the activation energy, against the solution obtained by a numerical shooting procedure described in the next section. Note that the quality of the approximation actually depends on the largeness  $\theta/c_s^2$ , which appears in the exponent of the Arrhenius term. For  $\gamma = 1.2$ ,  $c_s^2 \sim 1/10$  and excellent agreement is obtained for rather modest values of the activation energy.

Finally figure 3 shows the exponential sensitivity of the activation energy on the  $D_n - \kappa$  relation. For this plot we plotted the relation in the equivalent of dimensional scales. We chose a reference curvature,  $\kappa_{ref}$  and held all parameters fixed, such as  $\tilde{k}, \tilde{Q}, \gamma$ , and varied only  $\tilde{E}$ , or equivalently  $\theta$ .

## 4.2 The numerical shooting procedure

The exact (numerical) solution for the  $D_n - \kappa$  relation was calculated for finite curvature and activation energy. Since the basic result is a nonlinear eigenvalue problem, it can be solved by a relatively standard shooting algorithm as described below.

In the first step of the procedure, we fixed all the parameters in the master equation and boundary conditions, except for  $D_n$  and  $\kappa$ . Then we chose a particular value of  $\kappa$ , with certain limits. In general  $\kappa$  cannot exceed a critical value, which has been shown to depend strongly on the activation energy. We used the asymptotic formula to give an approximate range of  $\kappa$ .

Then we made a first guess of  $D_n$ . We refined this further by splitting the domain into two parts. We first used the analysis of the asymptotic formula to decide the approximate location of the turning point of the  $D_n - \kappa$ . To obtain a point on the upper branch of the  $D_n - \kappa$  curve we select a  $D_n$  bigger than the critical value of  $D_n$ , from asymptotic formula. To get a point on the lower branch we selected a  $D_n$  smaller than that critical value. The asymptotic formula gave an accurate first guess for  $D_n$ .

Next we were able to locate the CJ point, from the generalized CJ conditions, since  $\Phi$  and  $\eta$  are algebraic in  $U$  and  $\lambda$  and we used Newton-Raphson method for doing this. We started the integration in the  $U - \lambda$  plane moving in the correct direction, which requires a local linear analysis in the neighborhood of the generalized CJ point, which has a saddle character. By taking the Taylor series expansions of  $\Phi$  and  $\eta$  at the CJ point we obtained a quadratic equation for the slope  $dU/d\lambda$ . One of the two roots of this equation gives the proper slope at the CJ point.

A subroutine IMSL library, DIVPAG was used to integrate the master equation from the CJ point to the shock surface ( $\lambda = 0$ ) to determine the value of  $U$  at  $\lambda = 0$ . The correct value of  $D_n$  is obtained, when the value from integration matches the value of  $U(0)$  from the boundary condition  $U(0) = -D_n(\gamma - 1)/(\gamma + 1)$ . In general the first guess of  $D_n$  did not agree with the shock condition. However we defined a difference as a function of  $D_n$ , say  $f(D_n)$ . A Newton-Raphson method was then used to iterate on  $f(D_n)$  to find the root of  $f$ . This procedure converged and in turn defined  $D_n$  for a given value of  $\kappa$ . In all our calculations, we used double precision which allowed us to calculate case for relatively large activation energies.

## Acknowledgments

This work has been supported by the United States Air Force, Wright Laboratory, Armament Directorate, Eglin Air Force Base, F08630-92- K0057, and with computing resources from the National Center for Supercomputing Applications (NCSA).

## References

- [1] Stewart, D. S. and Bdzil, J. B., "The shock dynamics of stable multi-dimensional detonation", *Combustion and Flame*, 72, 311-323 (1988).
- [2] Bdzil, J. B. and Stewart, D. S., "Modeling of two-dimensional detonation with detonation shock dynamics", *Physics of Fluids*, A, Vol. 1, No. 7, 1261-, (1988).
- [3] Bdzil, J. B., Fickett, W. and Stewart, D. S., "Detonation Shock Dynamics: A new approach to modeling multi-dimensional detonation waves", *Proceedings of the 9th (International) Symposium on Detonation*, Portland, OR, 730-742. (1990).
- [4] Lee, J., Person, P. and Bdzil, J. B., "Detonation shock dynamics of composite energetic materials", submitted for publication.
- [5] Stewart, D. S., and Bdzil, J. B., "A lecture on detonation shock dynamics", *Lecture Notes in Physics*, 299, 17- 30, Buckmaster, J. D., Takeno, T., eds. Springer-Verlag (1988)
- [6] Klein, R. and Stewart, D. S., "The relation between curvature and rate state-dependent detonation velocity", *SIAM Journal of Applied Mathematics*, in press, to appear, Oct 1993.
- [7] Fickett, W. and Davis W. C., *Detonation*, California Press, (1979).
- [8] Wood, W. W. and Kirkwood, J. G. "Diameter effects in condensed explosives: The relation between velocity and radius of curvature", *Journal of Chemical Physics*, 22: 1920-1924 (1954).

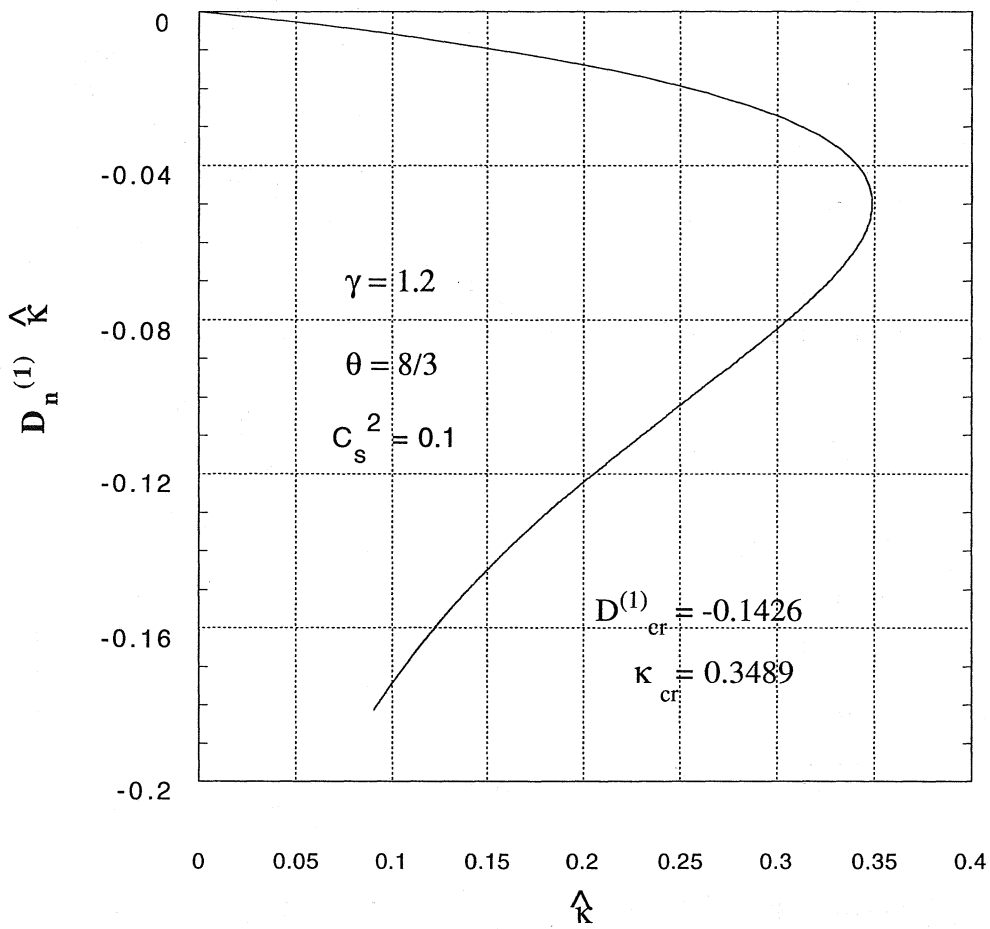


Figure 1:  $\hat{\kappa}$  versus  $\hat{\kappa}D^{(1)}$  from (18), for  $\gamma = 1.2$ . The formula illustrates the existence of a critical value of  $\kappa$ .

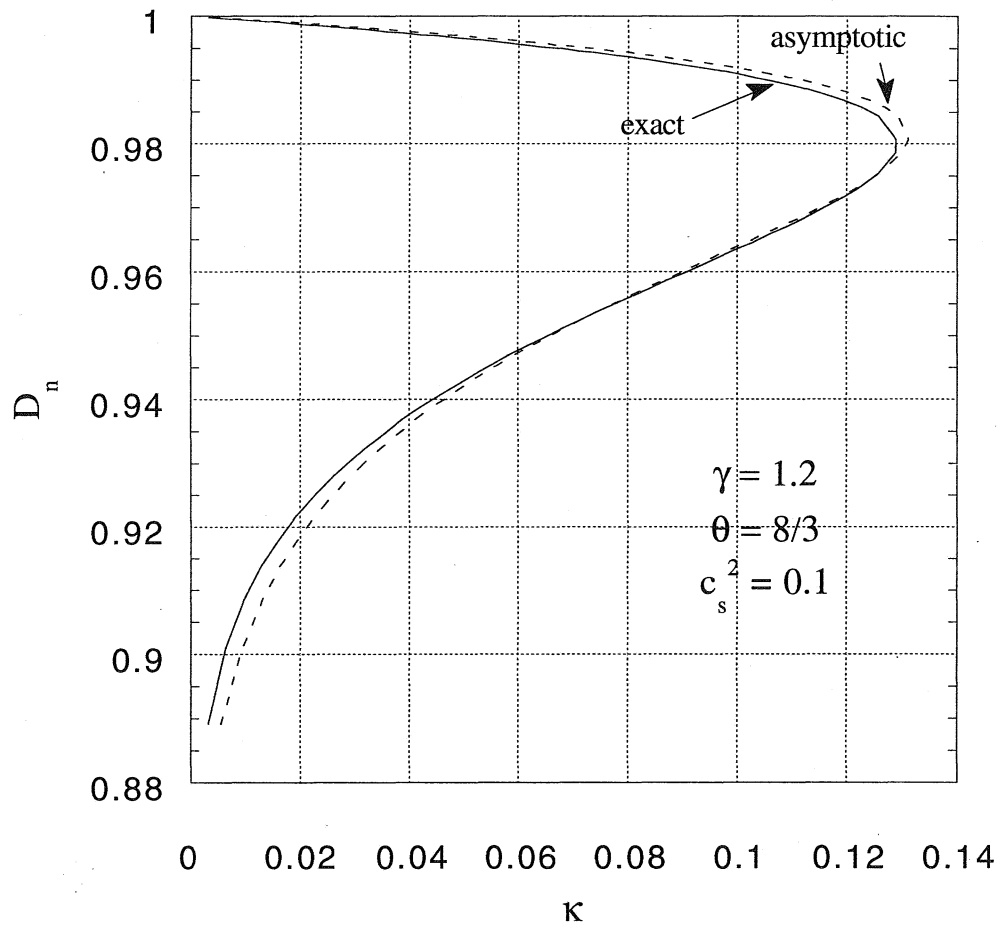


Figure 2: Comparison of the asymptotic and the numerically computed  $D_n - \kappa$  relation shown for  $\gamma = 1.2, c_s^2 = 0.1, \theta = 8/3, \theta/c_s^2 = 26.67$ . The numerical solution is plotted in the solid line, the asymptotic formula is plotted in the broken line.



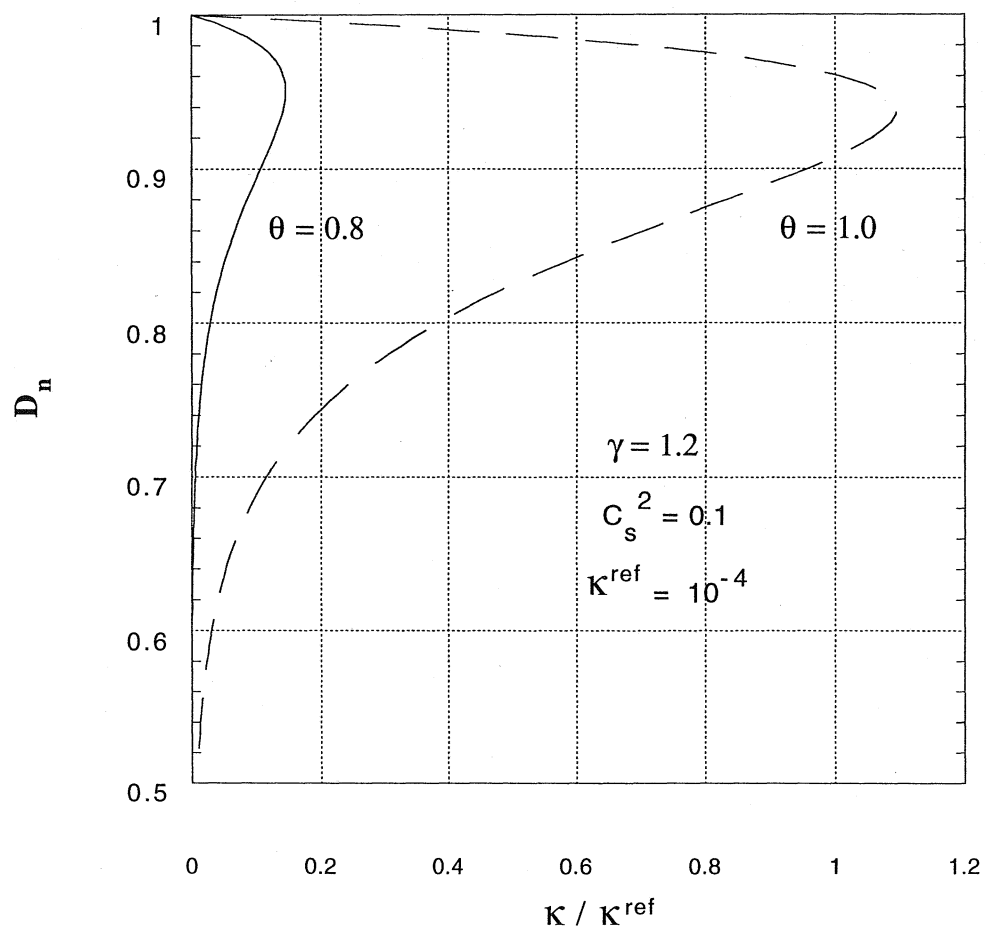


Figure 3:  $D_n$  versus  $\kappa/\kappa_{ref}$  to show the exponential sensitivity of the response to changes in the activation energy.  $\gamma = 1.2, c_s^2 = 0.1, \kappa_{ref} = 10^{-4}$ .



## List of Recent TAM Reports

No.	Authors	Title	Date
701	Bernard, R. T., D. W. Claxon, J. A. Jones, V. R. Nitzsche, and M. T. Stadtherr	Twenty-eighth student symposium on engineering mechanics, M. E. Clark, coord. (1991)	Apr. 1992
702	Greening, L. E., P. J. Joyce, S. G. Martensen, M. D. Morley, J. M. Ockers, M. D. Taylor, and P. J. Walsh	Twenty-ninth student symposium on engineering mechanics, J. W. Phillips, coord. (1992)	May 1992
703	Kuah, H. T., and D. N. Riahi	Instabilities and transition to chaos in plane wakes	Nov. 1992
704	Stewart, D. S., K. Prasad, and B. W. Asay	Simplified modeling of transition to detonation in porous energetic materials	Nov. 1992
705	Stewart, D. S., and J. B. Bdzil	Asymptotics and multi-scale simulation in a numerical combustion laboratory	Jan. 1993
706	Hsia, K. J., Y.-B. Xin, and L. Lin	Numerical simulation of semi-crystalline Nylon 6: Elastic constants of crystalline and amorphous parts	Jan. 1993
707	Hsia, K. J., and J. Q. Huang	Curvature effects on compressive failure strength of long fiber composite laminates	Jan. 1993
708	Jog, C. S., R. B. Haber, and M. P. Bendsoe	Topology design with optimized, self-adaptive materials	Mar. 1993
709	Barkey, M. E., D. F. Socie, and K. J. Hsia	A yield surface approach to the estimation of notch strains for proportional and nonproportional cyclic loading	Apr. 1993
710	Feldsien, T. M., A. D. Friend, G. S. Gehner, T. D. McCoy, K. V. Remmert, D. L. Riedl, P. L. Scheiberle, and J. W. Wu	Thirtieth student symposium on engineering mechanics, J. W. Phillips, coord. (1993)	Apr. 1993
711	Weaver, R. L.	Anderson localization in the time domain: Numerical studies of waves in two-dimensional disordered media	Apr. 1993
712	Cherukuri, H. P., and T. G. Shawki	An energy-based localization theory: Part I—Basic framework	Apr. 1993
713	Manring, N. D., and R. E. Johnson	Modeling a variable-displacement pump	June 1993
714	Birnbaum, H. K., and P. Sofronis	Hydrogen-enhanced localized plasticity—A mechanism for hydrogen-related fracture	July 1993
715	Balachandar, S., and M. R. Malik	Inviscid instability of streamwise corner flow	July 1993
716	Sofronis, P.	Linearized hydrogen elasticity	July 1993
717	Nitzsche, V. R., and K. J. Hsia	Modelling of dislocation mobility controlled brittle-to-ductile transition	July 1993
718	Hsia, K. J., and A. S. Argon	Experimental study of the mechanisms of brittle-to-ductile transition of cleavage fracture in silicon single crystals	July 1993
719	Cherukuri, H. P., and T. G. Shawki	An energy-based localization theory: Part II—Effects of the diffusion, inertia and dissipation numbers	Aug. 1993
720	Aref, H., and S. W. Jones	Chaotic motion of a solid through ideal fluid	Aug. 1993
721	Stewart, D. S.	Lectures on detonation physics: Introduction to the theory of detonation shock dynamics	Aug. 1993
722	Lawrence, C. J., and R. Mei	Long-time behavior of the drag on a body in impulsive motion	Sept. 1993
723	Mei, R., J. F. Klausner, and C. J. Lawrence	A note on the history force on a spherical bubble at finite Reynolds number	Sept. 1993
724	Qi, Q., R. E. Johnson, and J. G. Harris	A re-examination of the boundary layer attenuation and acoustic streaming accompanying plane wave propagation in a circular tube	Sept. 1993
725	Turner, J. A., and R. L. Weaver	Radiative transfer of ultrasound	Sept. 1993
726	Yogeswaren, E. K., and J. G. Harris	A model of a confocal ultrasonic inspection system for interfaces	Sept. 1993
727	Yao, J., and D. S. Stewart	On the normal detonation shock velocity–curvature relationship for materials with large activation energy	Sept. 1993

